J Mater Sci: Mater Med (2007) 18:1691–1699
DOI 10.1007/s10856-007-3068-8

Doxorubicin eluting beads – 1: Effects of drug loading on bead characteristics and drug distribution

Andrew L. Lewis · M. Victoria Gonzalez · Simon W. Leppard · Joanna E. Brown · Peter W. Stratford · Gary J. Phillips · Andrew W. Lloyd

Received: 4 January 2006 / Accepted: 6 June 2006 / Published online: 5 May 2007

Abstract DC Bead^{TM} is a FDA cleared embolisation device for the treatment of hypervascular tumours and arteriovenous malformations. This product is currently evaluated in a number of centres in Europe as an embolic device for transarterial chemoembolisation (TACE). The beads consist of poly(vinyl alcohol) microspheres modified with sulfonic acid groups and are available at different size ranges varying from 100 to 900 μm in diameter. The beads were shown to actively sequester doxorubicin hydrochloride (dox) from solution in a time dependent upon the dose of the drug and size of the beads. Drug uptake was by an ion-exchange mechanism, and in the absence of other ions in solution, the beads could load a maximum of around 40 mg dox/mL hydrated beads, with >99% of drug being sequestered from the solution. A loading of 25 mg dox/mL beads was recommended as providing a practical therapeutic dose and optimum handling characteristics. There was a decrease in equilibrium water content of the beads with increasing dox loading, which resulted in a decrease in the average diameter of the beads and an increase in the compressive modulus. The deliverability properties, however, were not affected after drug loading. Using a variety of microscopic methods, the drug was shown to be distributed throughout the bead structure, but concentrated in the outer 20 μm surface layer, a feature related to the method of synthesis. This study characterises the properties of DC Bead loaded with dox with respect to important characteristics in embolisation and demonstrates the potential of this drug device combination for the treatment of hypervascular tumours such as hepatocellular carcinoma.

A. L. Lewis (✉) · M. V. Gonzalez · S. W. Leppard · J. E. Brown · P. W. Stratford
Drug Delivery Division, Biocompatibles UK Ltd, Farnham Business Park, Weydon Lane, Farnham, Surrey GU9 8QL, UK
e-mail: andrew.lewis@biocompatibles.com

M. V. Gonzalez · G. J. Phillips · A. W. Lloyd
Biomedical Materials Research Group, School of Pharmacy and Biomolecular Sciences, University of Brighton, Moulsecoomb, Brighton BN2 4GJ, UK

Introduction

Hepatocellular carcinoma (HCC) is the fifth most prevalent cancer with a worldwide incidence of some 500,000 new cases per year, three quarters of those being in Asia. The treatment that a patient will receive is determined according to a staging system classified by the advancement of the disease. Currently, the treatment of choice for early stage sufferers is resection of the tumour or liver transplant; for those with intermediate or advance disease, resection is no longer an option and a number of alternative therapies are available including chemotherapy, embolisation or palliative treatments [1]. Minimally invasive procedures are finding favour because of their quality of life advantages, and include techniques such as transarterial chemoembolisation (TACE), radiofrequency ablation and cryoablation. Of these procedures, two recent randomised clinical trials have shown that TACE results in significant survival benefits over palliative care in the treatment of intermediate stage HCC in both European and Asian patient populations [2–4].

Outcomes, however, are far from reproducible from hospital to hospital, as there is no standardised method of performing the procedure. In general, the tumour is imaged under angiography by the interventional radiologist (IR) and a guidewire is used to position a microcatheter, usually

superselectively, into the main artery feeding the tumour. A chemotherapeutic agent (or mixture of agents) is administered intra-arterially, more often than not as an oily emulsion with an iodised contrast agent such as Lipiodol™ [5]. This metastable emulsion is viscous and slows the flow of blood in the target area. In a second step, an embolic agent is introduced into the artery to block the vessels completely and reduce wash-out of the chemo-emulsion. The choice of embolic agents is highly variable and can be biodegradable, such as gelatin foam, or permanent, including particulate or microspherical materials. Hence, with variations in technique, chemotherapeutic and embolic agent type and size, it is little wonder that results are inconsistent.

The success of drug-eluting stents has heralded the advent of combination devices that promise to deliver significant clinical benefits [6]. In this paper we describe the performance of a new drug device combination, the drug-eluting bead (DEB). This product was developed with an objective of standardising conventional TACE, providing handling advantages for the IR, whilst benefiting the patient with a reduction in side affects by sustained local delivery of chemotherapeutics directly to the tumour site [7]. The concept of delivering cytotoxic drugs from an embolisation matrix is by no means new in itself. Kerr and Kaye reviewed a number of systems utilising matrices based upon for instance, albumin, ethylcellulose and poly(lactic acid anhydride), for the delivery of drugs such as dox, mitomycin C and cis-platin among others [8]. Although promising during preclinical assessment, for various reasons the success of these systems did not seem to translate to the clinic [9].

DC Bead™ is a microspherical embolisation agent FDA cleared for the treatment of hypervascular tumours and arterio-venous malformations. It is composed of a poly(vinyl alcohol) (PVA) polymer hydrogel that has been modified by the addition of a sulfonic acid-containing component, and formulated by inverse suspension polymerisation into beads of varying size from 100 to 900 μm. The presence of the charged moiety enables the beads to interact with oppositely-charged drugs, such as doxorubicin hydrochloride (dox), the drug of choice in the treatment of a number of solid tumours including HCC. Here we describe the mechanisms of drug interaction with DC Bead™ and how the drug affects the properties of the bead with respect to important characteristics in embolisation. This paper describes a potential drug device combination, able to actively load therapeutically meaningful doses for use in the treatment of hypervascular tumours; further papers in this series will show how the bead modulates the release of the drug in a manner useful for local delivery and will correlate this release to that observed in-vivo.

Experimental

Materials

DC Bead embolisation microspheres (Biocompatibles UK Ltd, Farnham, UK) were supplied in sterile vials as 2 mL hydrated bead volume, suspended in 1 mmol sodium phosphate solution. Doxorubicin hydrochloride (dox, Dabur Oncology, UK) was obtained as a red powder (>99% purity) and dissolved in pure water to the desired concentrations.

Dox loading into beads

Beads were loaded with dox by immersion of a measured volume of beads into a drug solution of the desired concentration. In order to increase the efficiency of loading, it was found preferable to remove the sodium phosphate solution from the bead solution. This step was performed prior to loading by use of a syringe fitted with a 20G filter needle (B. Braun Medical, UK). The active uptake of the drug could be seen by the disappearance of the red colouration of the drug and change in bead colour from blue to deep red. Residual drug remaining in the depleted loading solution was determined by measuring the absorbance at 483 nm using a Perkin Elmer Lambda UV-Visible spectrophotometer and comparison to a standard curve constructed from solutions of known concentrations of drug.

Optical microscopy and bead sizing

The effect of drug loading on both the visual appearance and size of the beads was determined by use of an Olympus optical microscope fitted with video capture facility and Image-Pro Plus® (Media Cybernetics, Wokingham UK).

Fluorescence microscopy methods

Fluorescent microscope (FM) imaging of the drug-loaded beads was made using an Olympus Fluorescent Microscope Model BH-2 (Olympus Optical Co Ltd., Tokyo, Japan) and pseudo colour images were taken using the Starlight Xpress CCD Camera and Imagex software. Lenses of 40 × magnification and exposure time of 70 ms were employed to obtain best image quality.

Confocal laser scanning microscopy (CLSM) images were taken using a Zeiss LSM 410 confocal microscope, using the Argon 488 laser. A series of optical sections were recorded by moving the focal plane of the instrument 10 microns through the depth of the sample [10]. Different size ranges of beads (100–300 μm, 500–700 μm and

900–1200 μm) and different drug doses (5 mg/mL, 25 mg/mL and 45 mg/mL) were analysed.

Raman Fluorescent Microscopy (RFM) was performed using a standard LabRam 300 system, using 532 nm and 633 nm laser excitation. This system was equipped with a confocal Raman microscope and LabSpec software. The Raman spectra were acquired using 1-μm cross-section images [11].

Scanning Electron Microscopy (SEM) and Cryo-SEM

Scanning electron micrographs were taken using a Hitachi S-3500N SEM operated on secondary electron detection with an acceleration voltage of 5.00 kV. In some experiments the beads were fixed with glutaraldehyde before SEM analysis. This step was carried out to preserve their original shape. This was achieved by mixing the beads with 4 mL of 2% glutaraldehyde in phosphate buffered saline (PBS). The tubes were placed on roller mixers for 10–15 min and then the glutaraldehyde solution was removed, then the beads were washed 2 times with PBS and then 3 times with water. All bead samples were transferred onto sample SEM stubs, and placed in a desiccator overnight. Sputter coating with gold was performed prior to analysis using a Polaron SC502 sputter coater.

Beads of two size ranges (700–900 μm and 300–500 μm) were imaged using a LT7400 CT1500- cryo system mounted on a JEOL 6310 SEM. The samples were frozen using slushy nitrogen, fractured at –170 °C to expose the internal surface of the samples and then etched by heating to –70 °C to sublime the water on the surface. All samples were sputter coated with palladium before being returned to the SEM stage for imaging at –185 °C under 5 kV.

Measurement of bead water content

The water content of the beads was determined gravimetrically. It was expressed as the difference between the weight of the beads in the hydrated state and the weight of the beads after dehydration. A hydrated state was considered when excess solution was removed and the beads were left as a slurry. Dehydration was carried out by driving-off residual water using an oven at 80 °C. Initially, this process was carried out for 24 h, after that time every 8 h the vials were reweighed until no further decrease in mass was observed.

Measurement of bead compressibility

The compression test was performed using an Instron strength tensile tensor systems model 4411 fitted with a 50N load cell [12]. First, beads were spread on a flat surface to form a monolayer. The beads were then compressed 80% with a probe and the resistance to compression force was calculated. Only beads in the size ranges 700–900 μm and 900–1200 μm were found to be suitable for compression testing, as smaller beads did not generate reproducible results.

Determination of catheter deliverability

The bead deliverability test was assessed using 2.4 Fr (Progreat Terumo), 2.7 Fr (Progreat Terumo), 3 Fr (SP Radiofocus) and 4 Fr (Terumo) internal diameter (I.D.) micro/macro-catheters and the standard method used by doctors in clinical practice. This method was used for assessing deliverability before and after loading the beads. Each sample was mixed using 2 syringes and 3-way connectors with saline (0.9% $^{w}/_{v}$) and a contrast medium (Omnipaque 350) in a 50:50 ratio. When an even distribution of the beads was achieved, the test solution was delivered through a hydrated microcatheter. Both the ease of delivery and extent of clogging were scored according to a previously established scoring method [12]. Bead aggregation was scored No = 0, Yes = 1; catheter clogging was scored None = 0, Once = 1, Twice or More = 2; ease of injection was scored Easy = 0, Somewhat Difficult = 1 and Difficult = 2. The product was considered to fail deliverability if scoring 1 or 2 on catheter clogging and/or 2 for ease of injection. After delivery, the samples were visually checked, using the image analysis equipment, for shape recovery and fragmentation.

Results

Loading of dox into DC Bead

When a dox solution was added to a vial of DC Bead (in which the sodium phosphate solution had been removed to leave a slurry), the drug solution was seen to become depleted in colour and the blue beads turned red, as a result of drug loading (Fig. 1).

Figure 2 demonstrates that >99% of the targeted dose of dox was loaded in the beads, up to around a maximum of 40 mg of drug in a volume of 1 mL of hydrated beads; the immersion time, however, required to achieve this level of loading increased dramatically above 37.5 mg loading. The time taken to achieve maximum loading was also dependent upon the size of the beads, which is illustrated in Fig. 3 by use of a 25 mg dox solution with the beads sizes in the range 100–1200 μm. Here it was shown that the drug was taken-up into the beads very rapidly for the smallest bead size range (100–300 μm) such that complete loading was attained before the first sampling point at 10 min. The

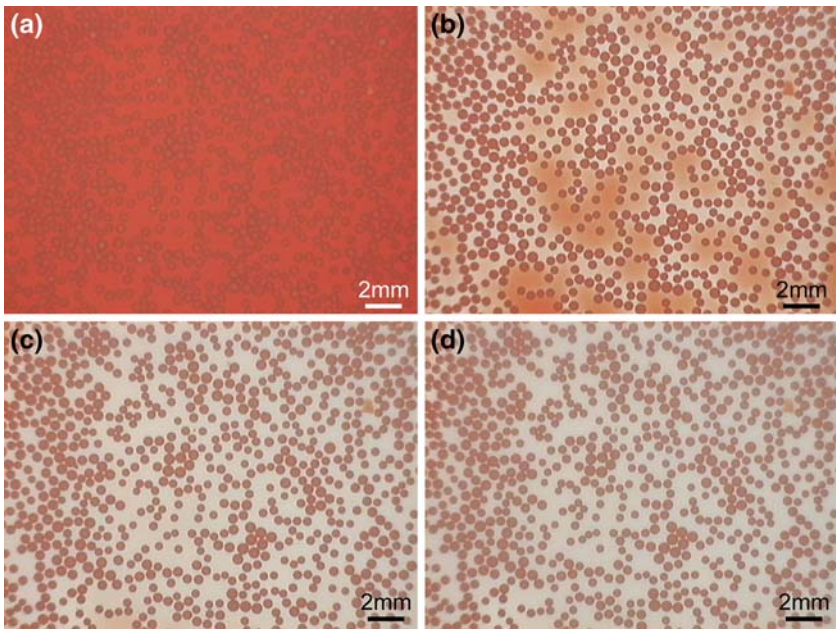

Fig. 1 Uptake of 25 mg dox by 1 mL beads over time (**a**) = 1 min; (**b**) = 10 min; (**c**) = 20 min; (**d**) = 60 min

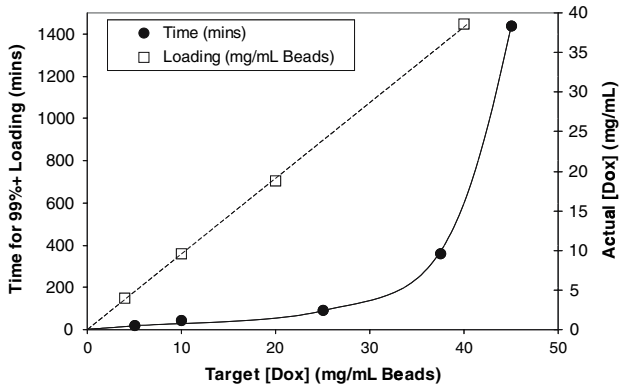

Fig. 2 Effect of [dox] on (**a**) actual loading achieved/mL beads; (**b**) time required to achieve >99% loading (mean, $n = 6$)

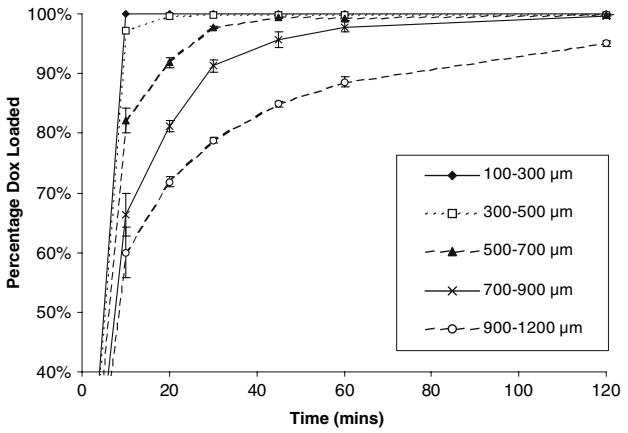

Fig. 3 Effect of beads size range on dox loading kinetics (mean ± s.d., $n = 3$)

loading process became progressively slower with increase in bead size; this could be explained as a result of a decrease in surface area as the bead size increases. The loading times are proportional to the surface area of the beads. All DC Beads in the commercially available sizes (100–900 µm) were loaded with 25 mg of dox/mL of beads within a maximum 2 h immersion period. The maximum loading of dox/mL beads was also determined for each of the bead size ranges. Statistical analysis using ANOVA showed that there was no significant difference between the maximum loading capacities of beads in any one size compared to another, the average maximum loading capacity for DC Bead being 39.0 ± 3.8 mg dox/mL beads.

Effect of dox loading on physical properties of the beads

Studies on the size distribution of the beads showed that increasing drug loading was accompanied by a concomitant decrease in the average diameter of the beads. Figure 4 reveals this effect across the commercially-available size ranges and shows the shift is far more pronounced in the larger beads compared to the smaller ranges.

The decrease in size is also accompanied by a drop in the equilibrium water content of the beads (Fig. 5). When unloaded and in pure water, DC Bead is a hydrogel material containing some 96% water. As the concentration of dox loaded into the beads was increased, the water content was seen to decrease, but was still at a level in the order of 85% at 45 mg/mL drug loading. This decrease in water content with increasing drug content was also accompanied by an increase in the resistance to

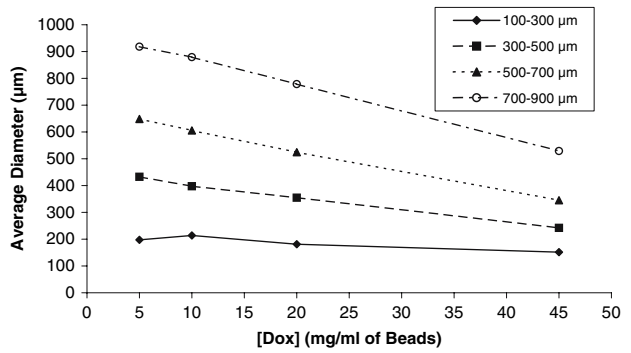

Fig. 4 Effect of [dox] on average diameter of beads in a particular size range (mean, $n = 3$)

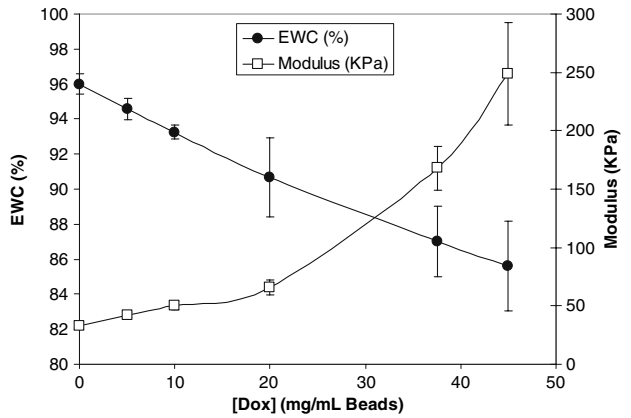

Fig. 5 Effect of [dox] on the EWC and resistance to compression of the beads (mean ± s.d., $n = 3$)

compression force of the beads (Fig. 5). The water content and compressibility of the beads were shown to return to the level of the unloaded DC Bead upon elution of all of the drug from the device.

The catheter deliverability test was performed using 2.4 Fr and 2.7 Fr microcatheters and 3 Fr and 4 Fr macrocatheters depending on the size of the samples analysed. All samples were analysed before and after loading with 25 mg of dox/mL of beads (as recommended by the manufacturer). Samples were mixed with saline and contrast medium (Omnipaque 350) in a 50:50 ratio to form the test solution. Prior to deliverability, the dox loaded beads were assessed for aggregation during mixing with water and the contrast medium. Bead aggregation was not observed in any of the delivery tests performed. All dox-loaded bead samples were delivered successfully *via* their designated catheters, being easy to inject and no catheter clogging observed (see Table 1). After delivery, all samples were visually assessed and all delivered samples remained spherical in shape with no fragmentation detected.

Investigation of dox distribution in the beads

Fluorescent microscopy was used to image 100–300 μm beads loaded with 25 mg dox/mL beads. The dox clearly fluoresced within the beads and showed an even distribution of drug across the surface with no visible inhomogeneity (Fig. 6). Cross-sectional analysis of the fluorescence intensity revealed nothing more than the spherical outline of the beads (see overlay on Fig. 6). Confocal laser microscopy was used to investigate the internal distribution of the drug by moving the focal plane throughout the depth of single beads loaded with different doses of dox. The intensity of the images produced was related to the concentration of the dox loaded. Figure 7 shows a gallery of confocal images in which (a) to (i) represent progressive sections from the top of a bead, moving downward throughout its structure by 10 μm each section. The very top section (a) showed a homogeneous distribution and represents the outer layer; as the sections moved progressively deeper, the centre of the image became less intense (although there was still dox present), the fluorescence being concentrated in the outer 20 μm of the beads structure. Figure 7(j) represents a confocal image of a bead that was fragmented to reveal the internal structure prior to

Table 1 Deliverability of DC Bead across the commercial size ranges when loaded with 25 mg dox/mL beads

Size range	100–300 μm	300–500 μm	500–700 μm	700–900 μm	900–1200 μm
Catheter type	2.4 Fr (Progreat)	2.4 Fr (Progreat)	2.7 Fr (Progreat)	2.7Fr (Progreat) 4Fr (Progreat)	4 Fr (Progreat)
Catheter clogging	0	0	0	1 0	0
Easy of injection	0	0	0	1 0	0
Acceptance criteria	Pass	Pass	Pass	Fail Pass	Pass

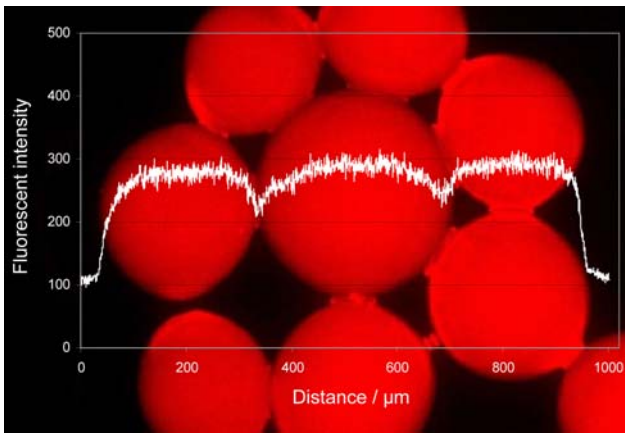

Fig. 6 Fluorescent microscopy image of dox-loaded beads (25 mg/mL 100–300 µm beads), 40 × magnification lens

immersion in a dox solution. Here again, there was a clear ring of fluorescence on the portion of the fragment that was from the outer regions of the bead

In order to rule out the presence of optical artefacts in the confocal images, the experiment was repeated using Raman fluorescent microscopy. Depth profiles were taken through the hydrated beads, monitoring the resulting fluorescence signal. A starting position was set (in this case, on the top surface of the bead) and a spectrum acquired. Through software control of the microscope sample stage height, the bead was moved into the second plane by a set amount (1 µm) and a further spectrum obtained. This process was repeated until the bead was fully analysed. Figure 8(a) shows the composite intensity profile for the unloaded DC bead, which shows an expected slope in intensity from the top to the bottom of the bead due to optical effects resulting in a weaker signal. The dox loaded bead shows intense regions at the bead surface (again, the signal at the bottom of the bead being correspondingly weaker) but confirming the confocal images and supporting the high-intensity fluorescence at the outer bead layers due to drug presence (Fig. 8 (b)).

Scanning electron microscopy analysis

The beads were imaged using SEM techniques. If hydrated beads were placed directly into the SEM chamber, the high

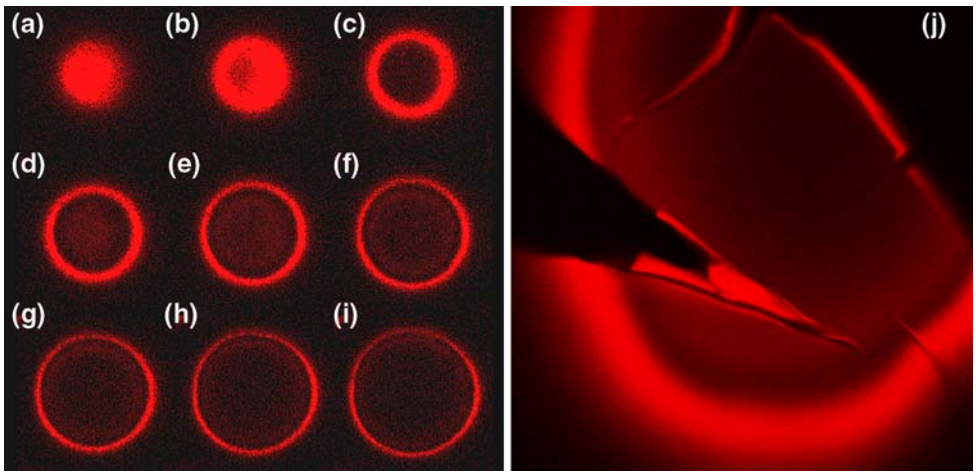

Fig. 7 Confocal laser scanning microscopy images of dox-loaded beads (25 mg/mL 500–700 µm bead) showing progressive sections from the outside inwards at 10 µm intervals (**a**)-(**i**). (**j**) Image of fractured section of bead revealing the drug distribution pattern

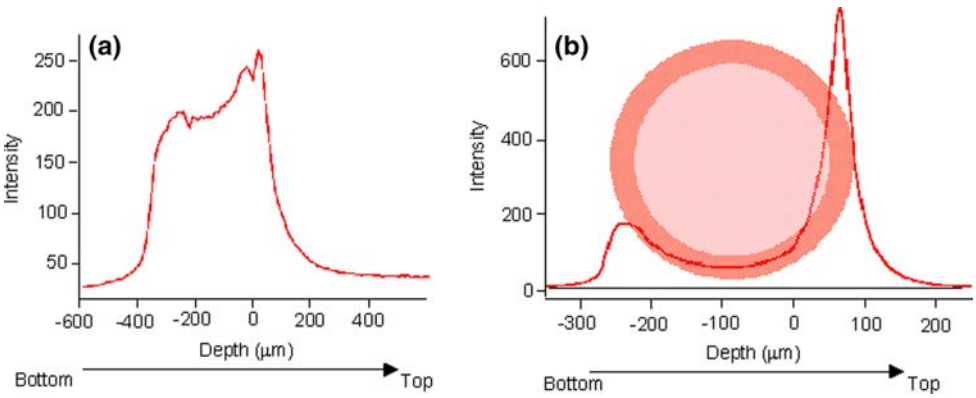

Fig. 8 Raman fluorescent microscopy depth profile of (**a**) an unloaded bead and (**b**) a dox-loaded bead (25 mg/mL 500–700 µm beads)

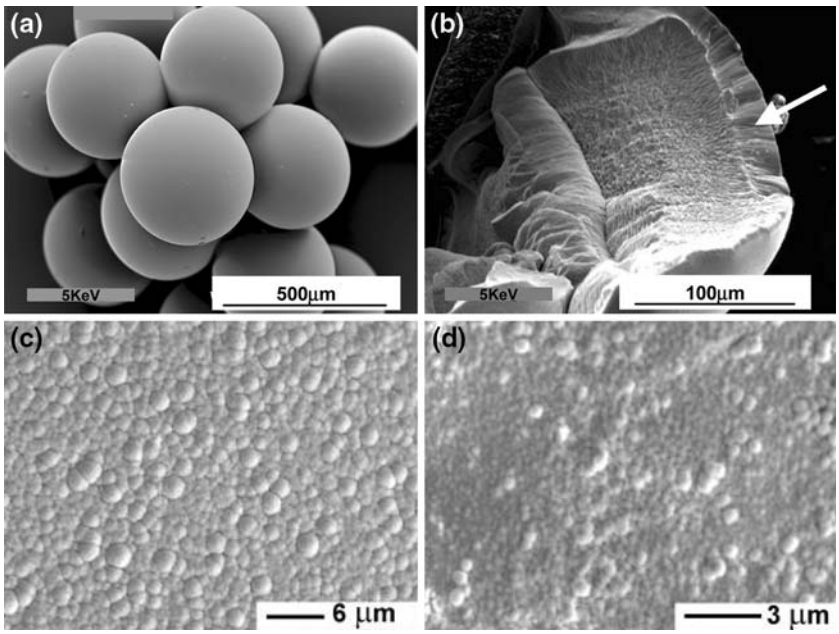

Fig. 9 (**a**) SEM of DC Bead (300–500 µm) fixed with glutaraldehyde; (**b**) internal image of unfixed bead revealing a dense outer skin (arrow); (**c**) Cryo-SEM image of the bead outer surface (300–500 µm); (**d**) Cryo-SEM of the bead inner surface

vacuum conditions resulted in rapid dehydration and collapse of the beads form, providing very little information on structure. Samples were therefore fixed with glutaraldehyde and Fig. 9(a) clearly shows the beads are uniformly spherical, smooth with no surface features visible, such as pores. An unfixed bead was sectioned, slowly dehydrated in a dessicator and imaged (Fig. 9(b)) which shows some internal structure to the bead. The internal core appears sponge-like, whereas the outer portion of some 20 µm in thickness appears to be a far more dense skin with little visible porosity. Cryo-SEM revealed little more of the gross structure but high magnification of the surface of the beads shows micron-sized spherulitic structures (Fig. 9(c)) and a similar internal structure to that on the surface except the spherical structures are sub-micron (Fig. 9(d)).

Discussion

DC Bead has been shown to actively sequester doxorubicin from solution, with a maximum bound capacity of around 40 mg/mL hydrated beads. From the clinical investigation of the treatment of HCC using DC Bead (by a procedure termed PRECISION TACE), it has been shown that the embolisation of a discrete tumour may require at least 4 mL of beads to produce adequate devascularisation [13]. Hence, a recommended dose of 25 mg/mL beads is suggested for the treatment of HCC using PRECISION TACE, typically resulting in a locally administered dose of 100 mg dox; this is thus below the recommended maximum 150 mg dox administered in any one procedure [14]. For the product to be practically usable in the clinic, it is required to load the drug over a relatively short time period. For bead sizes ranging from 100 to 900 µm, 25 mg dox/mL beads loads in less than 2 h, which an acceptable period from a clinical perspective as this process is carried out in the pharmacy prior to the embolisation taking place. Furthermore, smaller beads uptake dox much faster, which is related to the much greater surface area presented by the beads in solution and hence increased efficiency in absorbing the drug.

If a 25 mg dox solution is added directly to the DC Bead vial without first removing the sodium phosphate solution, the loading solution remains red and not all of the drug is sequestered (only 80%); whereas if the salt solution is removed, >99% of the dox is loaded. This is a result of the mechanism of interaction between the dox and the bead which is based upon ion exchange, similar to that reported for sulfonate-modified dextran microspheres reported by Liu [15]. Figure 10 (b) shows a schematic of the bead chemical structure and shows the presence of a significant proportion of sulfonate residues which act as a site for ionic interaction with the protonated primary amine group on the sugar moiety of the dox structure (Fig. 10 (d)). Interaction with the drug results in release of sodium chloride and also displaces some of the water in the hydration sphere around the ionic groups (Fig. 10 (c) + (d)). The high hydrophobicity of the drug will also contribute to the reduction of water content. As more dox is sequestered, more water is likely to be displaced with a loss of around 10% water content at maximum dox capacity of 40 mg/mL beads. The consequence of the loss of water is two-fold: the beads shrink, undergoing a decrease in their average diameter, again, an effect more pronounced in the larger beads

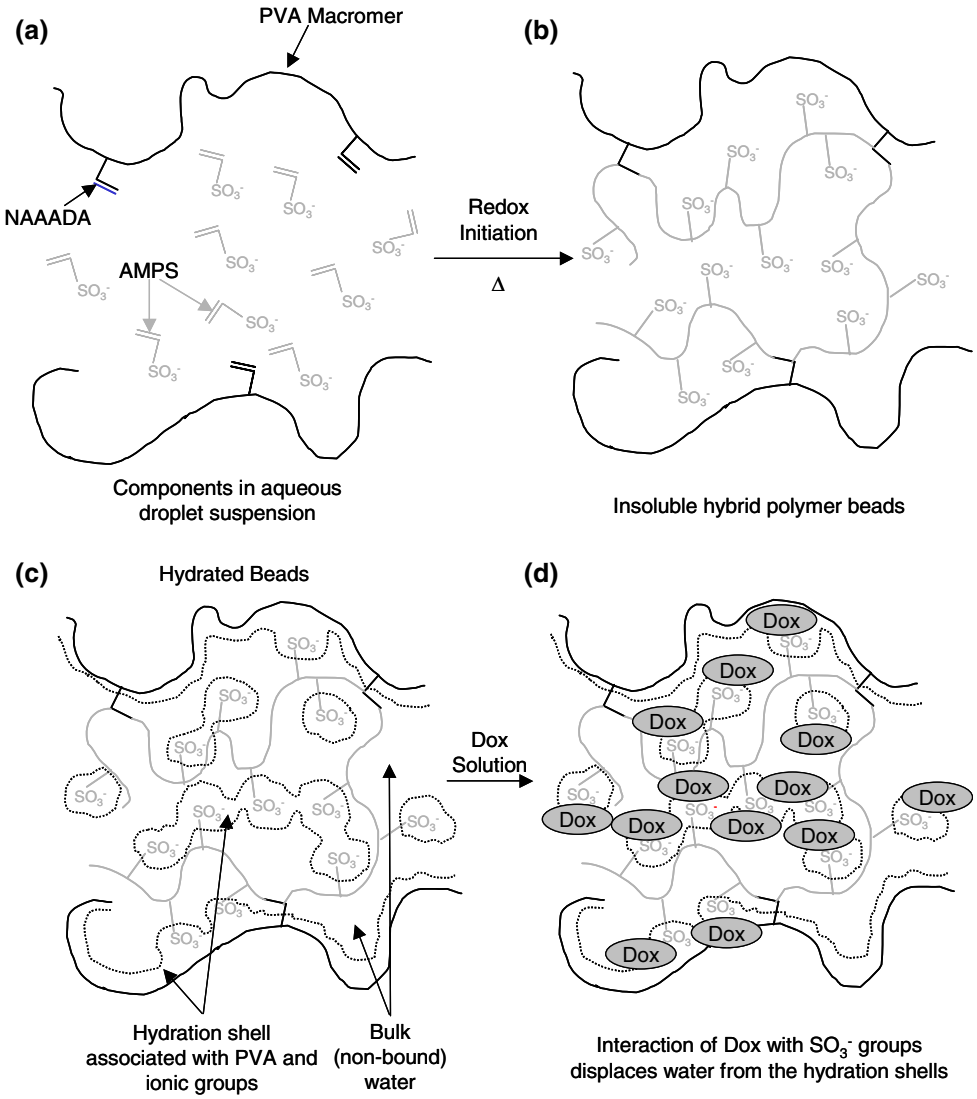

Fig. 10 Schematic for DC Bead (**a**) synthesis; (**b**) resulting chemical structure; (**c**) water-structuring within the hydrogel; (**d**) disruption of water structuring by dox interaction

because of the volume effects. Secondly, the loss of the plasticing effect of the water causes an increase in the modulus and makes the beads more difficult to compress [16]. These two points are crucial for embolisation agents, as the size range of product is selected on the basis of the size of the vessel to be blocked and compressible microspheres are selected because they can be delivered through microcatheters without blocking the narrow lumens. All the samples tested in this study were delivered successfully *via* their designated catheters, being easy to inject and no catheter clogging observed. Again, 25 mg/mL beads offers a good combination of characteristics and results in a product that can be delivered across the size range with characterised size shifts for the larger products.

In order to understand the distribution pattern of the drug in the beads, there is a need to appreciate the basics of their synthesis. The beads are produced by the inverse suspension free-radical polymerisation of a proprietary PVA-based macromer (modified with *N*-acryloyl-aminoacetaldehyde dimethylacetal, NAAADA) with 2-acrylamido-2-methylpropanesulfonate sodium salt (AMPS) [17]. The aqueous macromer/monomer mixture is suspended in butyl acetate and stabilised by cellulose acetate butyrate to prevent coagulation. Potassium persulfate is used as one half of a redox initiator couple, which is present in the aqueous phase. The stirred mixture is heated to 60 °C and then tetramethylethylenediamine (TMEDA, the other component of the redox couple) is added to the oil phase, where upon polymerisation is initiated and a water-swollen crosslinked network formed (Fig. 10 (a)). The beads are tinted blue using Reactive Blue 4 dye in order that they can be seen during use and then undergo various extraction processes to remove residuals. Finally, they are steam sterilised and packaged prior to use.

The result is a swollen hydrogel bead of ~95% water content, but with a high ionic content due to the AMPS.

This means the beads can undergo ion exchange, and in doing so, can effect water content, size and mechanical properties. There is no visible porous nature to the external surface of the beads by SEM, and even by the use of cryo-SEM in order to retain the hydrated structure, there are no clearly discernable structures externally, only micron-sized spherical ice crystals that have formed as the bead has been frozen. Fluorescent microscopy of the dox loaded beads also suggests a uniform distribution of drug on the surface, and hence a homogeneous distribution of the AMPS groups. The internal distribution as revealed by both confocal laser microscopy and Raman fluorescent microscopy is, however, not uniform, with the outer portion of the beads showing a higher concentration of drug. This can be rationalised by considering the synthetic process. Polymerisation of AMPS within the water phase is initiated by a redox reaction that occurs at the surface of the beads when the TMEDA diffuses through the oil phase to the surface of the aqueous persulfate-containing droplets. It is reasonable to expect that as the radicals are generated here, the AMPS monomer will begin to polymerise from the outside inwards. This may result in a region in the outer layer of the beads that is more dense than the inner portion, and hence will contain more AMPS content and thus more capacity to bind dox. This is confirmed by the SEM of a fragmented bead (Fig. 9 (b)) in which the internal structure is exposed and clearly shows a more dense skin some 20 μm in thickness on the outer portion of the bead (arrow), compared to a less dense, more spongey structure in the centre. The 20 μm thickness also correlates well with the fluorescent band measured by the confocal and Raman techniques.

Conclusions

DC Bead is an embolisation device FDA cleared for the treatment of hypervascular tumours and AVMs and which is currently being evaluated in a number of clinical centres in Europe for the one-step PRECISION TACE of HCC. Here we have described the simple method by which therapeutically-meaningful doses of dox can be loaded into DC Bead for use in clinical practice. Uptake of dox is an active ion-exchange process that can result in >99% drug loading in a few hours, dependent upon drug concentration and bead size. This is important clinically, as upon delivery of the beads into the hepatic artery, virtually all of the dox will be bound to the beads and none left in solution to enter into the general circulation where it can have significant toxicity-related side effects.

Dox uptake also results in changes in the physical parameters of the bead such as size and resistance to compression, which can be related to the displacement of water from the structure and have been well characterised. A loading of 25 mg dox/mL beads is recommended as providing a good balance of handling properties for the drug-device combination in clinical practice and offers a more than adequate therapeutic dose for local delivery. The beads have been shown to load the drug throughout the structure but more concentrated in the outer 20 μm of the surface, a phenomenon related to the synthesis method of the beads.

Naturally, for the drug-device combination to be effective, the dox must be released from the beads in a controlled fashion over a suitable time frame. The methods used to evaluate dox elution, detail on factors affecting the kinetics of dox release and in-vitro : in-vivo correlation are the subjects on a further follow-up paper by us on this device [18].

Acknowledgments VG would like to thank Biocompatibles UK Ltd for funding her PhD. Thanks also to Dr. Simon Fitzgerald, from LabRam Laboratories, for use of the Raman Fluorescent Microscope and Dr. Jin Hai Wang, from Biocompatibles UK Ltd, for use of the fluorescent microscope.

References

1. J. M. LLOVET, *J. Gastroenterol*. **40**(3) (2005) 225
2. J. BRUIX, M. SALA and J. LLOVET, *Gastroenterology* **127**(5 Suppl 1) (2004) S179
3. J. M. LLOVET, M. I. REAL, X. MONTAŇA, et al., *Lancet* **359** (2002) 1734
4. C-M. LO, H. NGAN, W-K. TSO, et al., *Hepatology* **35** (2002) 1164
5. M. S. CHEN, J. Q. LI, Y. Q. ZHANG, et al., *World. J. Gastroenterol.* **8**(1) (2002) 74
6. A. L. LEWIS and M. J. DRIVER, *Eur. Biophram. Rev.* (Summer) (2005) 82
7. A. L. LEWIS, M. V. GONZALEZ, A. W. LLOYD, et al., *JVIR* **17**(2) (2006) 335
8. D. J. KERR and S. B. KAYE, *Crit. Rev. Ther. Drug Carrier Syst.* **8**(1) (1991) 19
9. P. M. J. FLANDROY, C. GRANDFILS and R. J. JEROME, *Pharmaceutical particulate carriers: Therapeutic applications*, edited by A. Rolland (Marcel Dekker Inc: New York 1993) p. 321
10. A. LAMRECHT, H. YAMAMOTO, H. TAKEUCHI and Y. KAWASHIMA, *J. Control Release* **90**(3) (2003) 313
11. H. R. MORRIS, C. C. HOYT and P. J. TREADO, *Appl. Spectrosc.* **48**(7) (1994) 857
12. A. L. LEWIS, C. ADAMS, W. BUSBY, *et al.*, *J. Mater. Sci: Mater. Med.* **17** (2006) 1193
13. Personal communications with J.Bruix, the Barcelona Clinic for Liver Cancer, Barcelona, Spain
14. E. A. LEFRAK, J. PITHA, S. ROSENHEIM and J. A. GOTTLIEB, *Cancer* **32** (1973) 302
15. Z. LIU, R. CHEUNG, X. Y. WU, *et al.*, *J. Control Release* **77** (2001) 213
16. W-I. CHA, S-H. HYON, O. MASANORI and Y. IKADA, Mechanical and wear properties of poly(vinyl alcohol) hydrogels, Macromolecular Symposia 109 (36th Microsymposium on Macromolecules High-Swelling Gels, 1995) (1996) 115
17. D. W. GOUPIL, H. HASSAN, T. HOLLAND, *et al.*, Embolic compositions comprising polymers with a diol structure unit. WO 2001068720 (Biocure Inc)
18. M. V. GONZALEZ, Y. TANG, G. J. PHILLIPS, *et al., J. Mater. Sci: Mater. Med.* in press